SPECTRORADIOMETER INTER-COMPARISON OF PAR, UV AND ALL WAVELENGTH QUANTUM SENSORS

Sylvio L. Mantelli Neto[1,2], Daniele C. dos Santos[2], Marília Braga[2], Thamires A. Silva[2], and Ricardo Rüther[2]

[1] INPE Brazilian National Institute for Space Research, São José dos Campos SP, Brazil

[2] UFSC Federal University of Santa Catarina, Florianópolis SC, Brazil

Abstract

This study utilizes a spectroradiometer (SPR) capable of selective bandwidth removal, allowing for paired comparisons of independent data sources. The data analysis focused on clear sky conditions (CSC) and quantum sensors to evaluate their performance and calibration. It was observed that there is a high correlation among the ultraviolet (UV), Photosynthetically Active Radiation (PAR), and reference cell (RC) data compared to the SPR readings. The analysis indicated that sensors tend to overestimate the data due to an excess of smooth transitions in the spectral bands, in contrast to the sharp transitions integrated by the SPR. The best comparison was with the UV sensor, attributed to the high quality of its dome. The PAR sensor, which also showed a good correlation, demonstrated a strong influence of seasonal data and should be further evaluated in a more complex experiment using exogenous parameters. The reference cell (RC) showed the smallest correlation due to the lower quality of its flat surface designed to mimic a mono-crystalline solar module. Nevertheless, it still provided a good correlation and curve fitting, with lesser influence from seasonal conditions, and could be used for calibration comparisons with a similar bandwidth, even with a less sensitive angular response.

Keywords: Spectroradiometer, inter-comparison, validation, PAR, UV and RC.

1. Introduction

PAR, UV, and RC sensors are used in monitoring stations and low-cost applications. PAR is an important parameter in studies of the conversion of solar energy into chemical energy used by plants Proutsos et al. (2022). UV is frequently employed in various degradation processes and has erythemal impacts on the population. RCs are widely used to monitor solar irradiation in photovoltaic (PV) plants due to their similar spectral response of mono crystalline solar module. PAR, UV, and RC data can be obtained directly from quantum sensors (QS) or derived from empirical models based on piranometers associated with exogenous parameters Jacovides (2010), Noriega et al. (2020). Two technologies commonly used in solar sensors are thermopiles and QS. High-grade piranometers are thermopile-based and suitable for wide waveband monitoring of global, direct, and diffuse solar irradiation. Quantum sensors, which are photo-diode based, have a limited wavelength range but offer a fast response and can be used for selective wavebands such as UV, PAR, RC, and spectroradiometer (SPR) applications. Although thermopiles have a wider spectral response, they exhibit a slower signal response and do not allow for selective wavelength applications. In contrast, QS can provide a better description of energy distribution. While piranometers also have a wide spectral response, their performance is affected by local climate conditions such as clouds, aerosols, humidity, and solar position, which can introduce uncertainties detrimental to precise research. Quantum sensors like UV, PAR, and RC, may not offer the same wide spectral range, but they have a fast response time and are more selective, enabling the observation of spectral distribution under varying air mass conditions and atmospheric compositions (EKO MS-711 manual, 2015 p. 8). SPRs are available at several monitoring sites. Although SPRs are more expensive and involve complex operations and data integration, their band selectivity can be utilized to inter-compare and calibrate dedicated QS, as both types of sensors are photo-diodes. This work proposes to inter-compare similar bands selected from a SPR with those of PAR, UV, and RCs. Preliminary, we will perform an exploratory data analysis (EDA) to compare data under clear sky conditions to minimize the effects of clouds and random atmospheric variability.

10.18086/swc.2025.04.44 Available at http://proceedings.ises.org

2. Material and methods

The data utilized in this study were obtained from a digital EKO MS-711 SPR, which collected measurements every minute. Additionally, analog sensors from KIPP&ZONEN (K&Z) including the PQS1-PAR and CUV5-UV, alongside a RC from INGENIEURBÜRO Si-02-Pt100 for ALL band. Data from the analog sensors were recorded by a CAMPBELL CR3000, providing 1-minute averages for 1-second sampling. A statistical analysis was conducted using a pair comparison for every 1-minute temporal resolution data. Only data collected from 8-22 GMT were used. Numerical integration on SPR data was used to compare the power among the sensor bands. To convert PAR energy the SPR data from radiant units (W/m^2) to chemical energy (Photosynthetic Photon Flux Density or PPFD, in $\mu mol/m^2.s$), we applied the conversion factor of 4.47 ± 0.1, as determined by McCree (1972, 1981) within the waveband of 400-700 nm (McCree 1971). The CUV5-UV data (280-400 nm) was compared against the MS-711 data (300-400 nm). For the exploratory data analysis (EDA), nine clear sky days during the sunlight period were manually selected from June 27th or day of year (DOY) 179, July 1st and 2nd or DOYs 183, 184, August 11th, 13th, 14th, 26th, 27th, 30th or DOYs 224, 227, 239, 240 respectively, and November 11th or DOY 316 of 2024. Identifying perfectly clear skies in our climate is challenging due to atmospheric instability and seasonal variability and the data set was limited to 9 days. We based the clear sky selection from a EKO sky imager and K&Z global (SMP22), direct (SHP1) and diffuse (SMP22) piranometers. The binomial distribution present on Figures 2-4 is due to a mid-spring clear day of year (316) on data sample. These days provided 4,613 comparison points, which the authors believe offer sufficient statistical significance for the analysis.

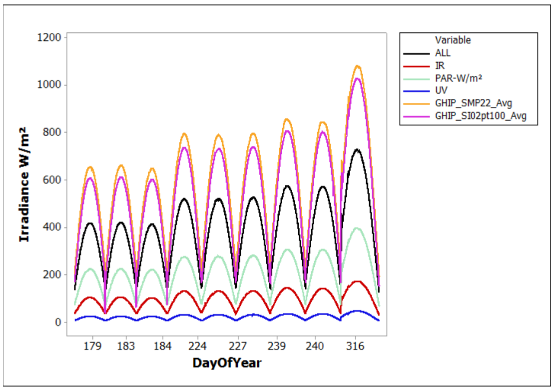

Fig. 1: Pyranometer, quantum sensors and SPR clear day data used in the present work along the year.

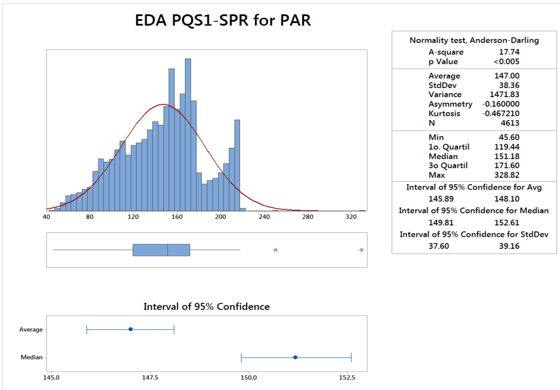

Fig. 2: Statistical summary of pair differences between quantum PQS1 and SPR data for PAR.

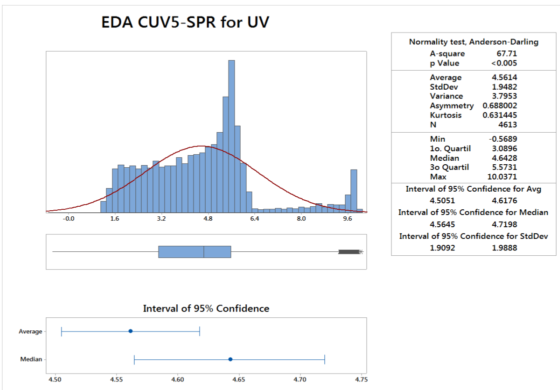

Fig. 3: Statistical summary of pair differences between quantum CUV5 and SPR data for UV.

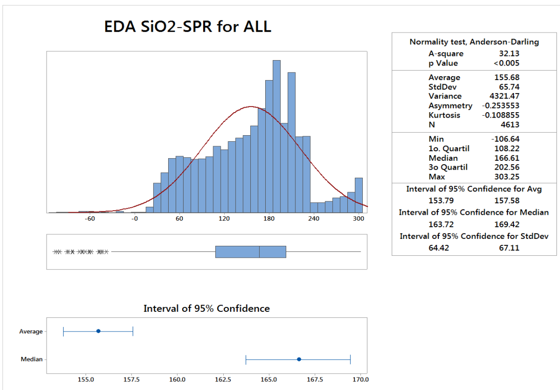

Fig. 4: Statistical summary of pair differences between quantum SiO2 and SPR data for All spectral range.

All the sensors were deployed at the same date and the degradation along time is considered the same for all QSs and SPR. Preliminary data used for this analysis along with one SMP22 Pyranometer data were illustrated in Figure 1. Figures 2-4 present the statistical summary of the pair differences between the quantum sensors (PQS1, CUV5, and SiO2) and their respective SPR bands (PAR, UV, and ALL). Table 1 provides the correlation coefficients and biases for clear sky conditions across the PAR, UV, and ALL bands.

Tab. 1: Correlation coefficients between quantum sensors and SPR wavelength bands for clear skies.

Wavelength band	Pearson correlation	Bias	Standard Deviation
PAR	0.995	147.00	38.36
UV	0.998	4.5614	1.9482
ALL	0.998	155.68	65.74

3. Conclusions

The data analysis indicated a bias in favor of QS due to their different spectral responses (McCree, ch. 2.6, 1981). Individual QS exhibit a wider spectral response with longer spectral leading and trailing transitions and minimal spectral mismatch than SPR. Under these conditions, differences in energy integration obtained by SPR are expected, as the wavelength separation of the bands is sharper and narrower compared to those of the QS. The data error showed a very small difference between the UV and SPR bands, as illustrated in blue on histogram of Figure 5. However, the differences were considerably larger for the PAR and ALL bands.

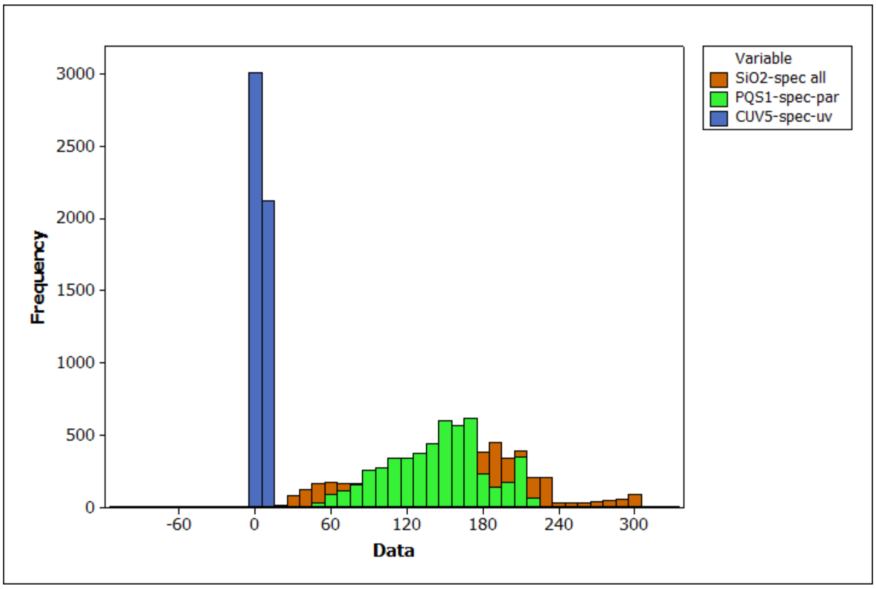

Fig. 5: Histogram of differences illustrating the pair comparison of SPR against PAR, UV, and ALL bands.

These differences are due to the quality of sensors' surfaces. CUV5 have a high quality quartz dome and a better cosine response similar to SPR. PQS1 use a teflon diffusor disk to improve the cosine response and SiO2 use flat PV module glass. Although it was found a high correlation among the sensors as indicated in Table 1, the data also indicated higher biases, variances, and also higher uncertainties for PQS1 and Si02 on the measurements. From these observations we can infer that the quality of sensor surface really makes a difference on sensor's uncertainty and variance.

On the dispersion graphs of figures 6-8 the Y-axis represents the differences between SiO2, PQS1 and CUV5 and their respective selected SPR bands against to solar zenith angle (θz). Four different months are illustrated according to the figure legends. As could be observed on these figures the differences reduces as θz increases, due to better angular response of SPR. On fig. 3, the PAR data is separated in 3 groups months 6 and 7 we collected in temporally the same winter clear sky days sequence like the other group on month 8. Month 11 is single day event on mid spring. These separated groups indicates seasonal exogenous influence in the atmosphere, that should be analyzed in a more complex experiment analysis. On fig. 7 the differences seems to be more scattered, but the vertical scale is nearly orders of magnitude smaller than figures 6 and 8. The data of month 11 on fog. 7 has that shape due to different atmosphere conditions of morning and evening periods of the day that could be better observed in small scales. This indicates that for more precise evaluation exogenous atmospheric contents like humidity, temperature, etc should be taken into account.

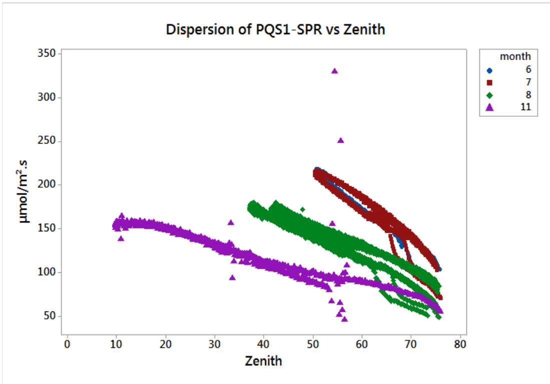

Fig. 6: Pair difference between PQS1 and SPR along the solar zenith angle for PAR.

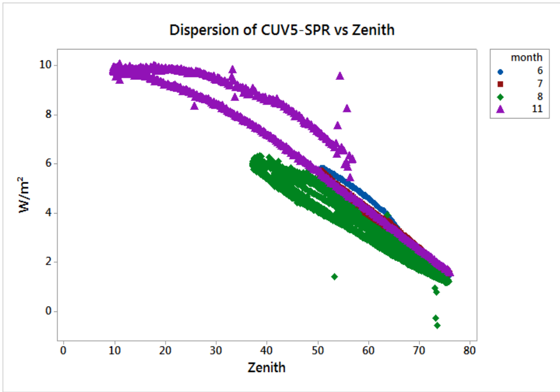

Fig. 7: Pair difference between CUV5 and SPR along the solar zenith angle for UV.

For fig. 8 all points seems to be scattered along one curve. There is also a non-linear difference reduction as θz increases meaning that SiO3 angular response degrades much more than SPR. From these observations means that a correlation exists between SPR and SiO2, and a single squared adjusted function could be used for calibration as described in eq. 1 and illustrated in fig. 9.

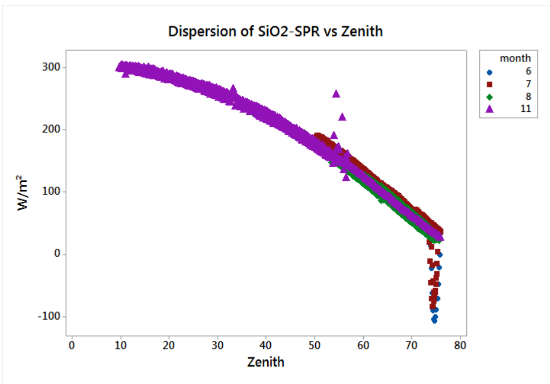

Fig. 8: Pair difference between Si)2 and SPR along the solar zenith angle for ALL bands.

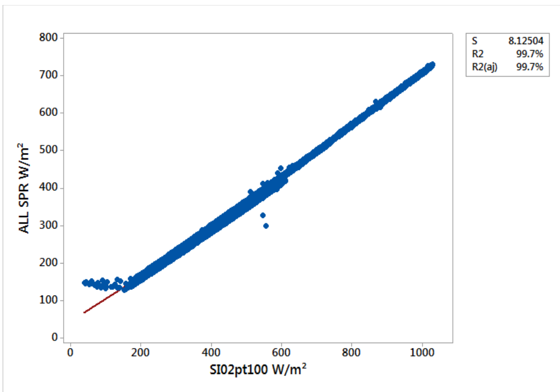

Fig. 9: Correlation between SPR and SiO2 for clear skies @ Florianópolis SC Brazil

$$SPR' = 44.79 + 0.5757\ SI02 + 0.000094\ SI02^2 \qquad \text{(eq. 1)}$$

Where:

SPR': is the irradiance data obtained by spectrum integration in W/m^2 , SiO2: is the irradiance data read from reference cell in W/m^2 .

For future work suggestions it is recomended to build up a data library of clear skyes to be used on a new improved model. For a different location it is necessary to repeat the experiment with local data under local atmospheric conditions. For PAR and UV sensors, it is necessary to consider exogenous data to improve the of the intercomparison of sensors sensitive to atmospheric variations or sazonal changes.

The analisys of this article help us to understand the empirical relations among the sensors, their limitations and and qualities. It helped us to build up a more apropriete method for calibration of RC based on SPR quantum sensors instead of Pyramoneters with a different spectral response.

4. Acknowledgments

This project was developed with support of SHELL BRAZIL PETRÓLEO in the project: MELHORIA DA EFICIÊNCIA ENERGÉTICA SOLAR
23080.007076/2022-32.

5. References

EKO Insrtruments CO. LTD. 2015. Spectroradiometer model MS-711 Instruction Manual version 1.0.

Jacovides, C., Boland, J., Asimakopoulos, D., Kaltsounides, N. 2010. Comparing Diffuse Radiation Models With One Predictor For Partitioning Incident PAR Radiation Into Its Diffuse Component In The Eastern Mediterranean Basin. Renewable Energy, Elsevier BV, 35, 1820-1827

McCree K. J. 1971. The action spectrum, absorptance and quantum yield of photosynthesis in crop plants. Agricultural Meteorology 9: 191-216. https://doi.Org/10.1016/0002-1571(71)90022-7

McCree KJ. 1972. Significance of enhancement for calculations based on the action spectrum for photo-synthesis. Plant Physiology 49: 704-706. https://doi.org/10.1104/pp.49.5.704

McCree, K.J.. 1981 Photosynthetically Active Irradiation. In: Physiological Plant Ecology I. Encyclopedia of plant physiology (Lange OL,, Nobel PS, Osmond CB, ZieglerH. Eds.) Springer Berlin 41-55. https://doi.org/10.1007/978-3-642-68090-8.3

Noriega Gardea, M. M. A., Corral Martínez, L. F., Anguiano Morales , M.; Trujillo Schiaffino, G., Salas. Peimbert, D.P. 2020. Modelling Photsynthetically Active Radiation: A Review Atmosphera, Centro de Ciencias de la Atmosphera,.

Proutsos, N. D., Liakatas, A., Alexandris, S. G., Tsiros, I. X.; Tigkas, D., Halivopoulos, G. 2022. Atmospheric Factors Affecting Global Solar and Photosynthetically Active Radiation Relationship in a Mediterranean Forest Site Atmosphere, MDPI AG, 13, 1207

McCree, K. 1981. J. Physiological Plant Ecology I, Springer Berlin Heidelberg,